Electronic Supplementary Information (ESI)

Immobilization of Ferrocene and Its Derivatives within Metal-Organic Frameworks with High Loadings toward Efficient Oxygen Evolution Reaction

Shulin Li,‡[b] Xiangyang Shangguan,‡[a] Zhaoxin Zhou,[b] Wenyue Niu,[a] Yajing Zhang,[a] Xiaonan Wang,[a] He Zhu,[b] Guoguo Liu,[a] Kangjun Wang[a,*] and Guangli Yu[a,*]

[a] College of Chemical Engineering, Shenyang University of Chemical Technology, Shenyang 110142, P. R. China. *E-mail:* yugl0507@163.com, wangkj_dut@syuct.edu.cn

[b] School of Science and Engineering, The Chinese University of Hong Kong, Shenzhen 518172, P. R. China

‡ These authors should be considered as co-first authors.

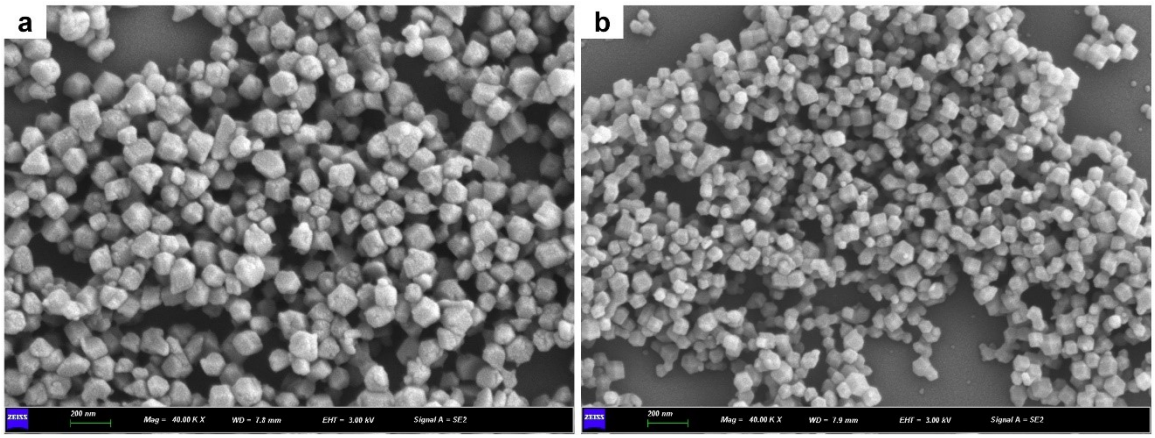

Fig. S1 SEM images of ZIF-8 (a) and Fc/ZIF-8-2:1 (b).

Table S1 Pore structure of ZIF-8 and Fc/ZIF-8-2:1.

Sample	S_{BET} ($m^2\ g^{-1}$)[a]	S_{micro} ($m^2\ g^{-1}$)[b]	V_{total} ($cm^3\ g^{-1}$)[c]	V_{micro} ($cm^3\ g^{-1}$)[d]
ZIF-8	1785.5	1672.2	1.75	0.62
Fc/ZIF-8-2:1	938.9	770.7	1.09	0.38

[a] Brunauer-Emmett-Teller (BET) surface area estimated at P/P_0 = 0.005-0.05, [b] microporous surface area determined by *t*-plot method at P/P_0 = 0.4-0.6, [c] total pore volume calculated at P/P_0 = 0.995, [d] micropore volume determined by *t*-plot method.

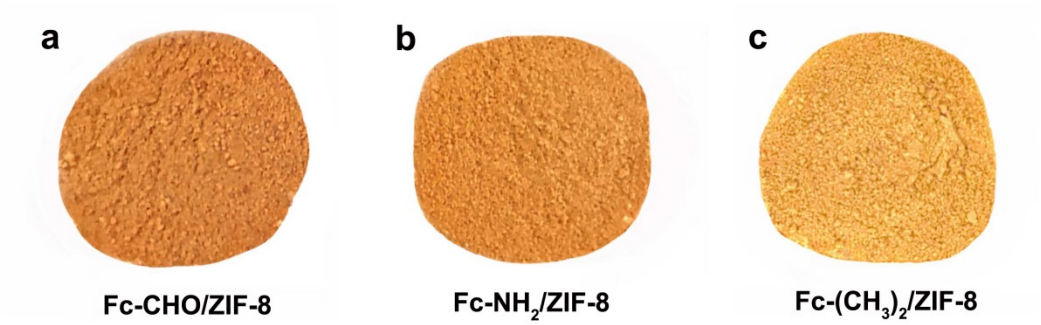

Fig. S2 Optical photos of Fc-CHO/ZIF-8 (a), Fc-NH_2/ZIF-8 (b) and Fc-$(CH_3)_2$/ZIF-8 (c).

Table S2 Content of Fe determined by ICP-AES in Fc-CHO/ZIF-8, Fc-NH_2/ZIF-8 and Fc-$(CH_3)_2$/ZIF-8 composites.

Sample	Fe (%)
Fc-CHO/ZIF-8	3.6%
Fc-NH_2/ZIF-8	3.5%
Fc-$(CH_3)_2$/ZIF-8	3.9%

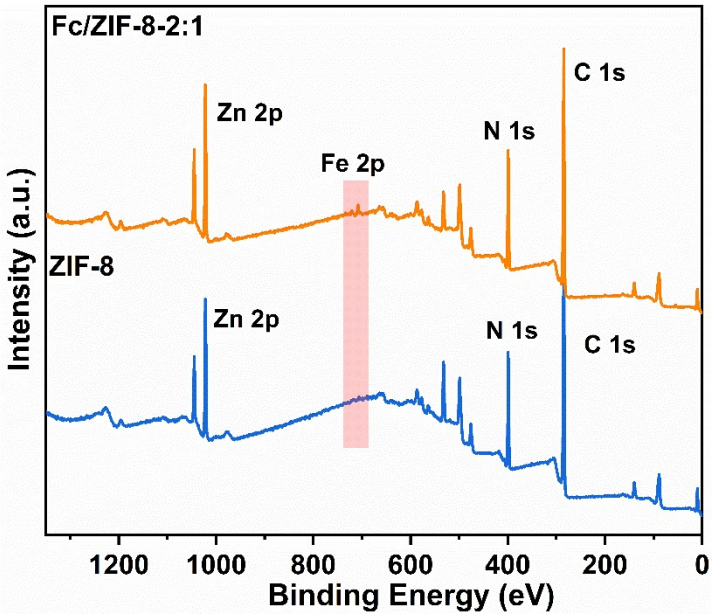

Fig. S3 XPS survey spectra of Fc/ZIF-8-2:1 and ZIF-8.

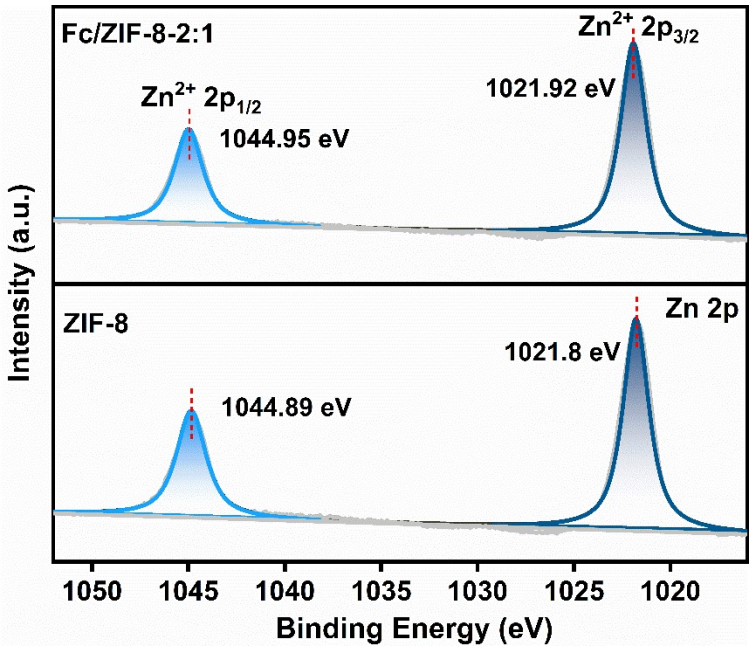

Fig. S4 High-resolution XPS spectra of Zn 2p in pristine Fc/ZIF-8-2:1 and ZIF-8.

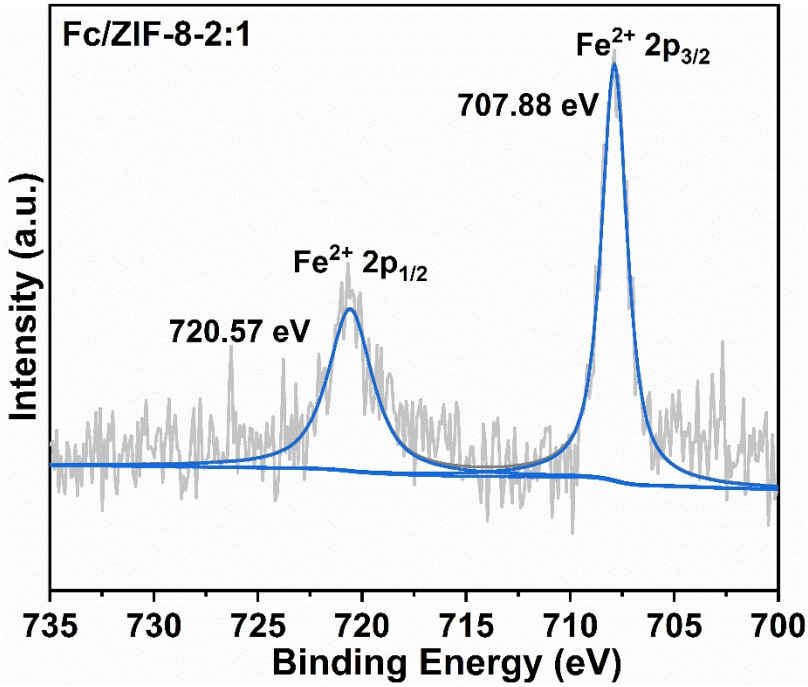

Fig. S5 High-resolution XPS spectra of Fe 2p in pristine Fc/ZIF-8-2:1.

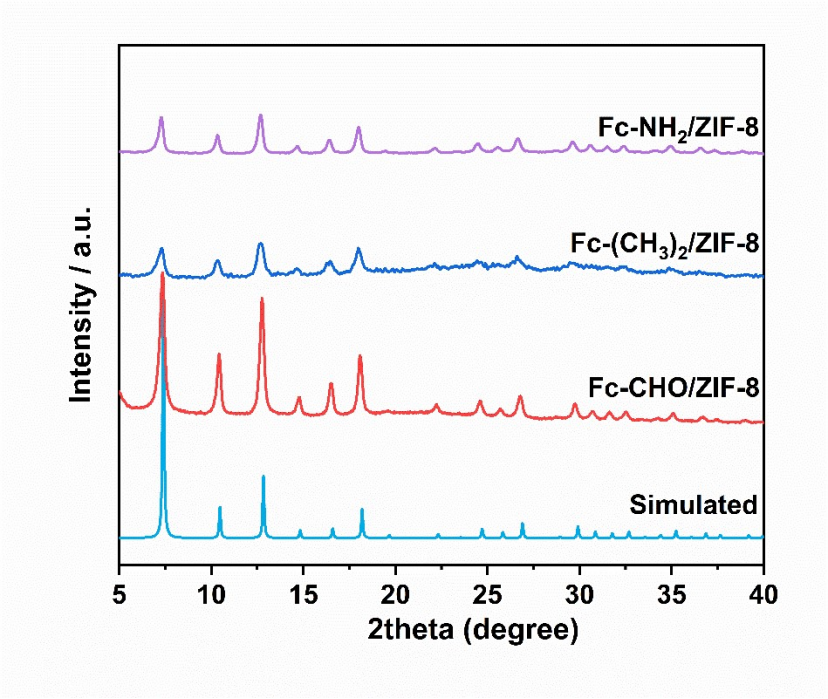

Fig. S6 XRD patterns of simulated ZIF-8, Fc-CHO/ZIF-8, Fc-$(CH_3)_2$/ZIF-8 and Fc-NH_2/ZIF-8.

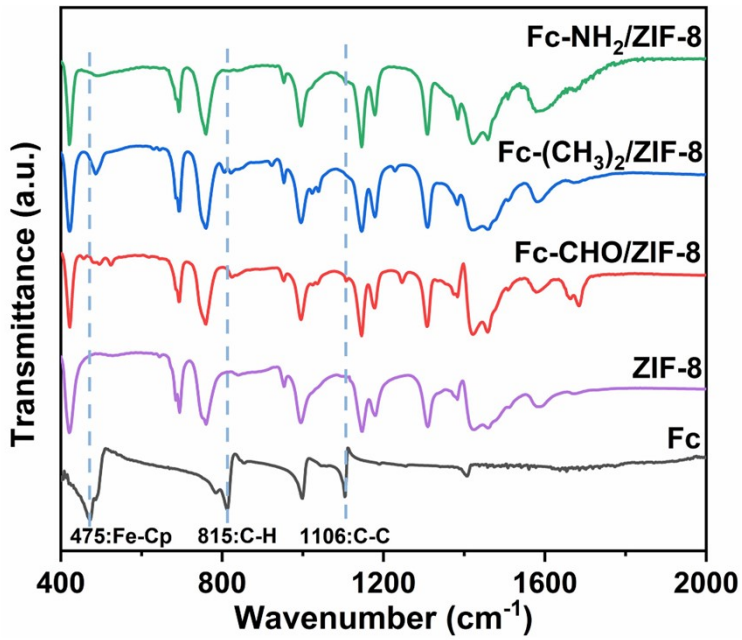

Fig. S7 FT-IR spectra of Fc, ZIF-8, Fc-CHO/ZIF-8, Fc-$(CH_3)_2$/ZIF-8 and Fc-NH_2/ZIF-8.

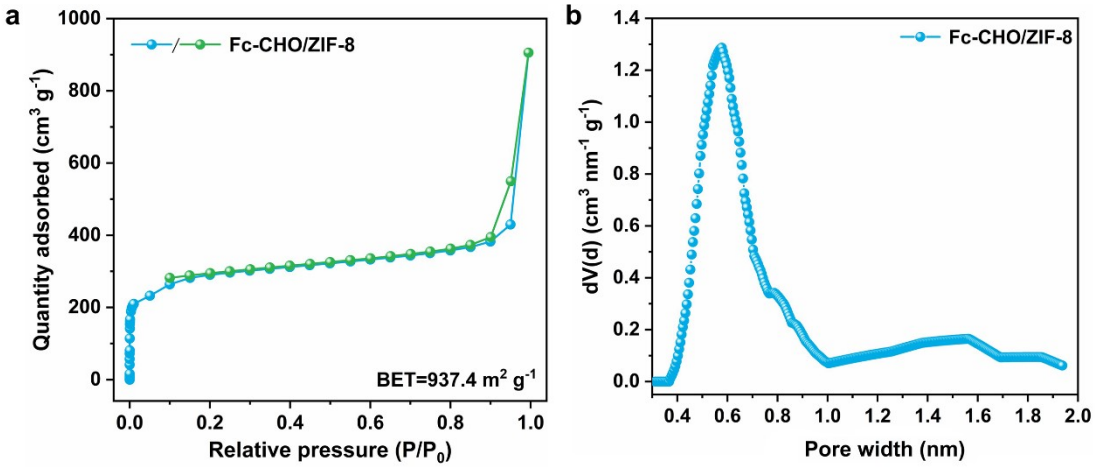

Fig. S8 N_2 adsorption-desorption isotherms (a) and the pore size distribution using the Horvath-Kawazoe model (b) of Fc-CHO/ZIF-8.

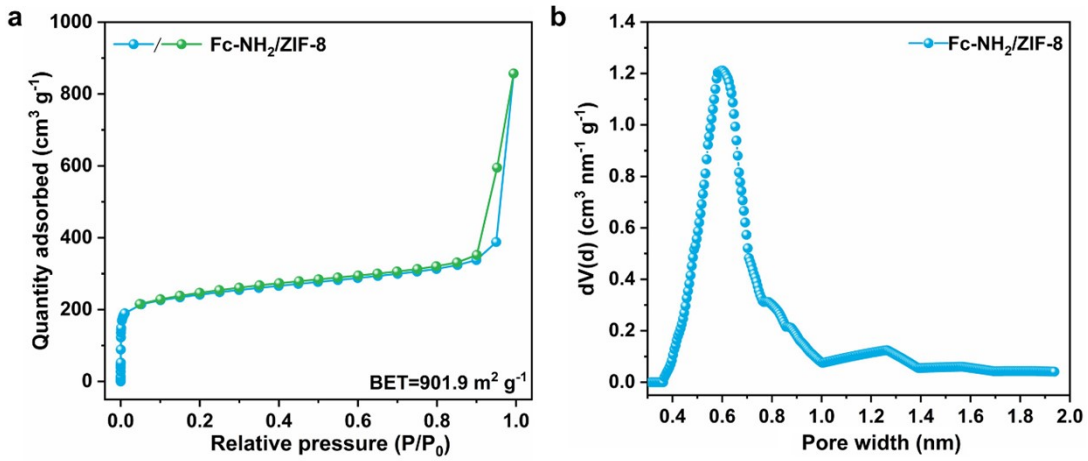

Fig. S9 N_2 adsorption-desorption isotherms (a) and the pore size distribution using the Horvath-Kawazoe model (b) of Fc-NH_2/ZIF-8.

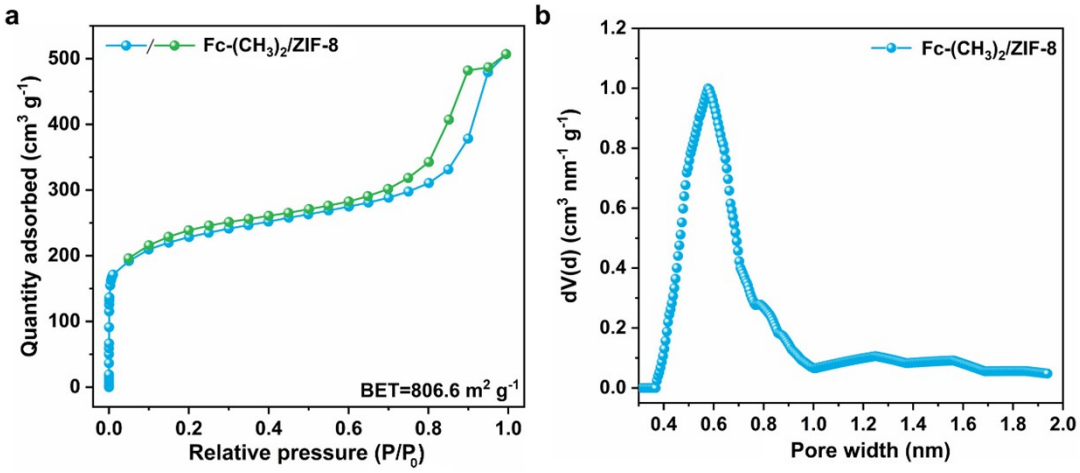

Fig. S10 N_2 adsorption-desorption isotherms (a) and the pore size distribution using the Horvath-Kawazoe model (b) of Fc-$(CH_3)_2$/ZIF-8.

Table S3 OER performances for this work and reported Fe/Co/Ni-based OER catalysts under alkaline conditions.

	Overpotential (mV) at 10 mA cm^{-2}	***Tafel slope (mV dec^{-1})***	***References***
Fc/ZIF-8	246	52	This Work
Fc*-CHO/*ZIF-8	238	44.4	This Work
BMM-10-Fe-H	260	137.4	1
NiFe-MOF NSs	240	73.44	2
G-FeNi-Co-ZIF-L/NF	248	49.5	3
Fe-Ni MOF NSs/NF	258	40.8	4
Co$_3$(HITP)	254	86.5	5
NiCoFeP	273	35	6
CoFe-MOF-NK	268	77.5	7
MCCF/NiMn-MOFs	280	86	8
CoNi1@C	276	55.6	9
CoCu-MOF	271	63.5	10
Ni-Co LDH@ZIF-67-V$_o$/NF	290	58	11
CoFeMOF	265	44	12
I^{3}O^0-type Co-MOF	361	28	13
Ni@NC	280	46	14
NiFc-MOF	195	44.1	15
FeTAPP-NiTCPP-POP	338	52	16
Co porphyrins 1/CNTs	407	60.3	17

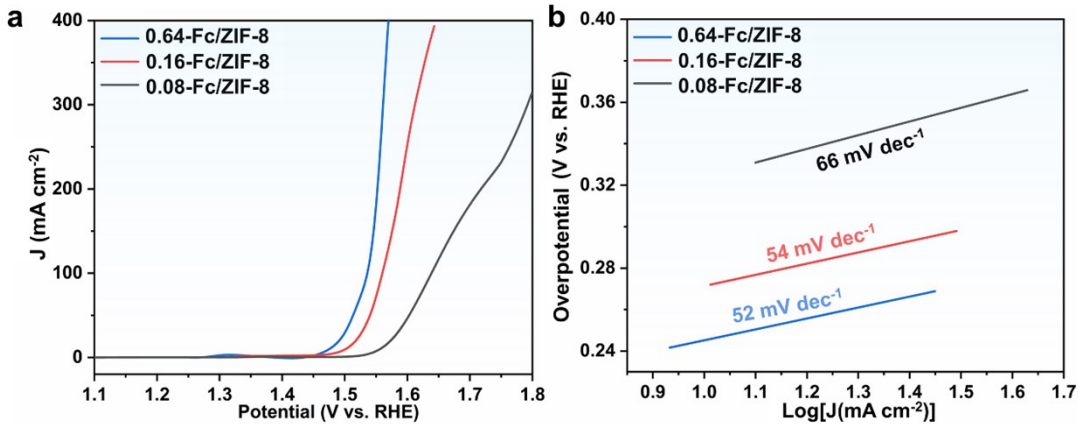

Fig. S11 LSV curves (a) and corresponding Tafel slopes (b) of Fc/ZIF-8 with different Fc loading.

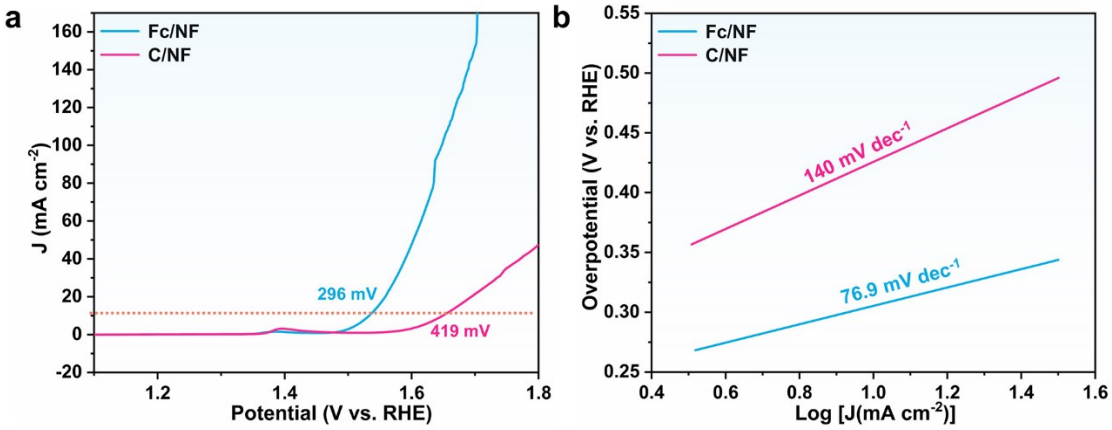

Fig. S12 LSV curves (a) and corresponding Tafel slopes (b) of Fc/NF and C/NF.

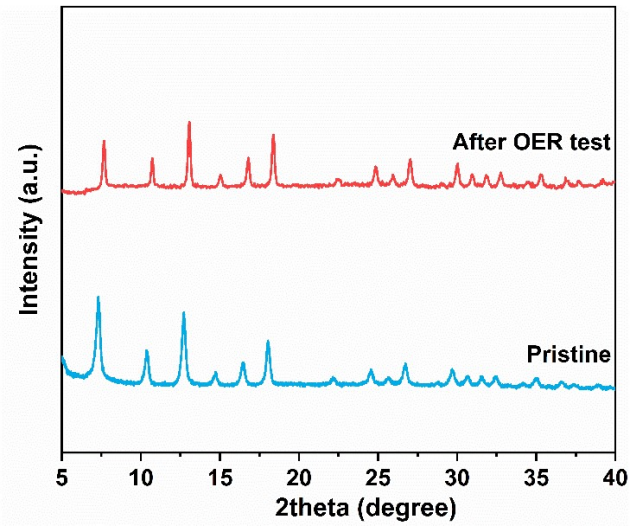

Fig. S13 XRD patterns of of Fc/ZIF-8 before and after OER test.

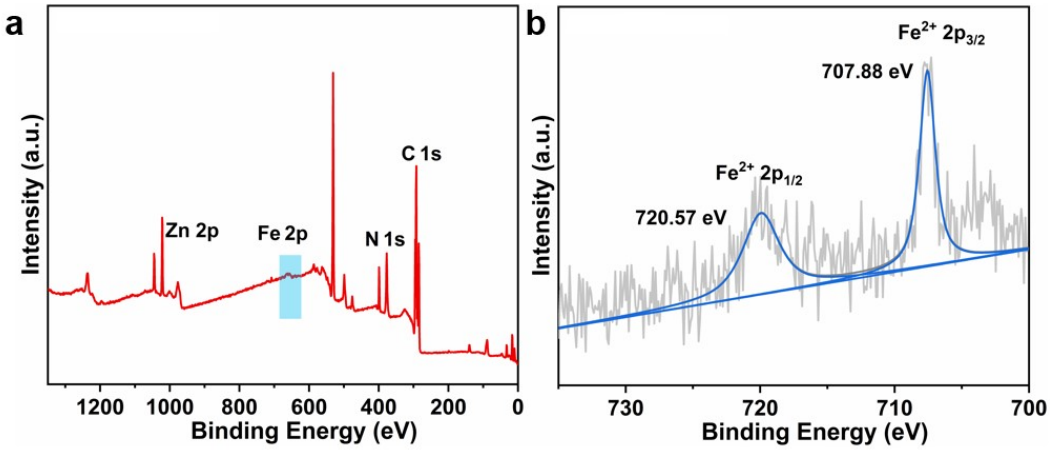

Fig. S14 XPS survey spectra (a) and Fe 2p (b) of Fc/ZIF-8-2:1 after OER test.

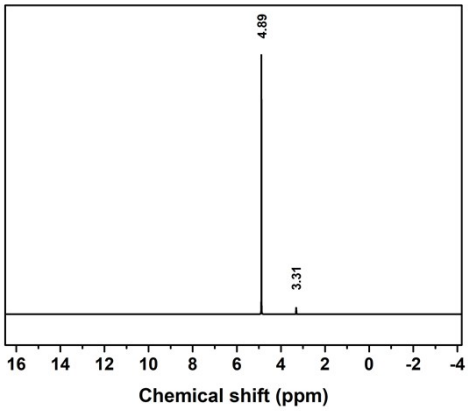

Fig. S15 1H NMR spectra of the electrolyte solution in methanol-d4 reagent.

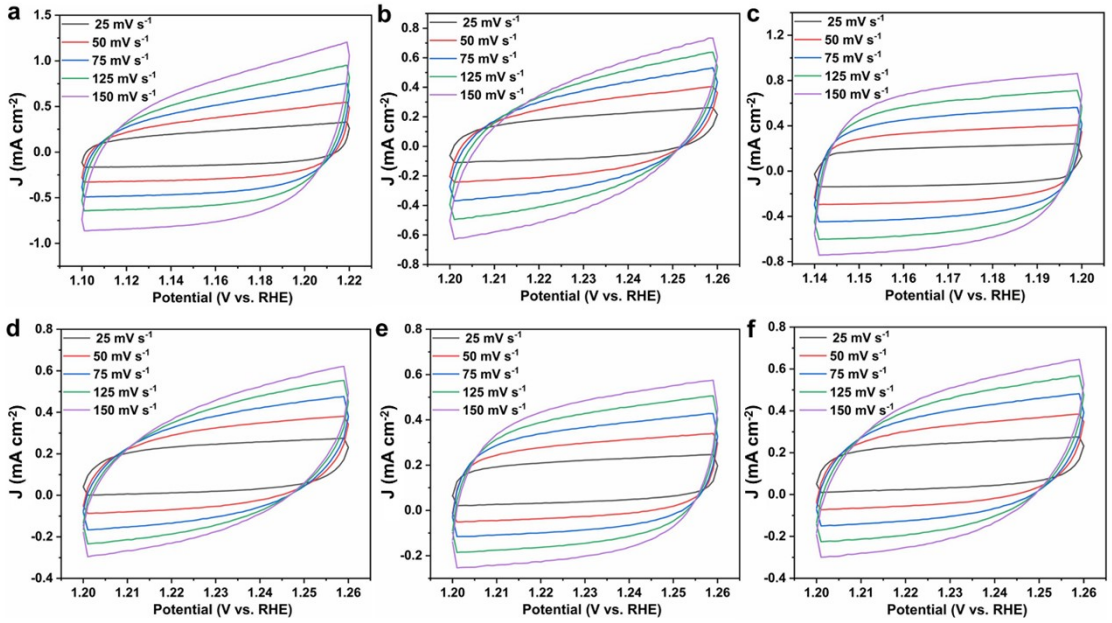

Fig. S16 CV curves measured at different scan rates of Fc/ZIF-8-0:1 (a), Fc/ZIF-8-1:1 (b), Fc/ZIF-8-2:1 (c), Fc/ZIF-8-3:1 (d), Fc/ZIF-8-4:1 (e) and ZIF-8 (f).

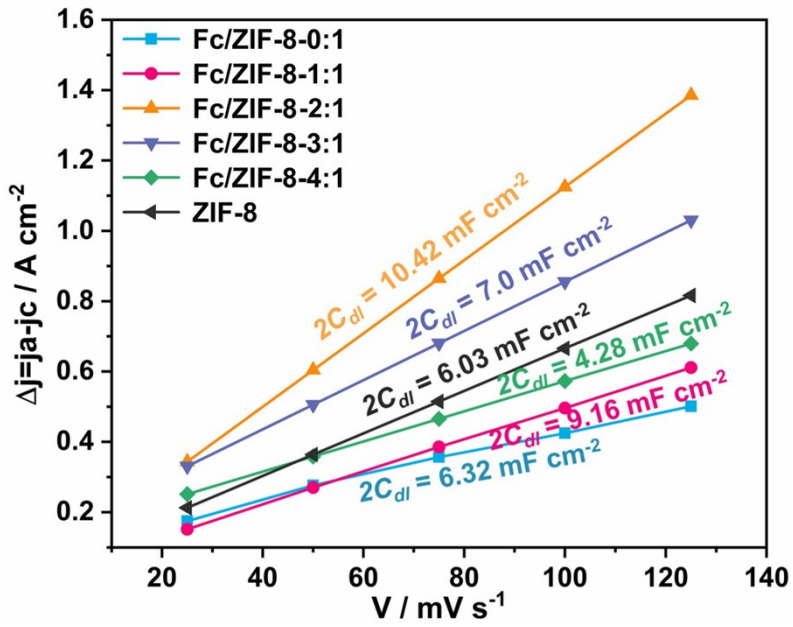

Fig. S17 C_{dl} values of Fc/ZIF-8-0:1, Fc/ZIF-8-1:1, Fc/ZIF-8-2:1, Fc/ZIF-8-3:1, Fc/ZIF-8-4:1 and ZIF-8.

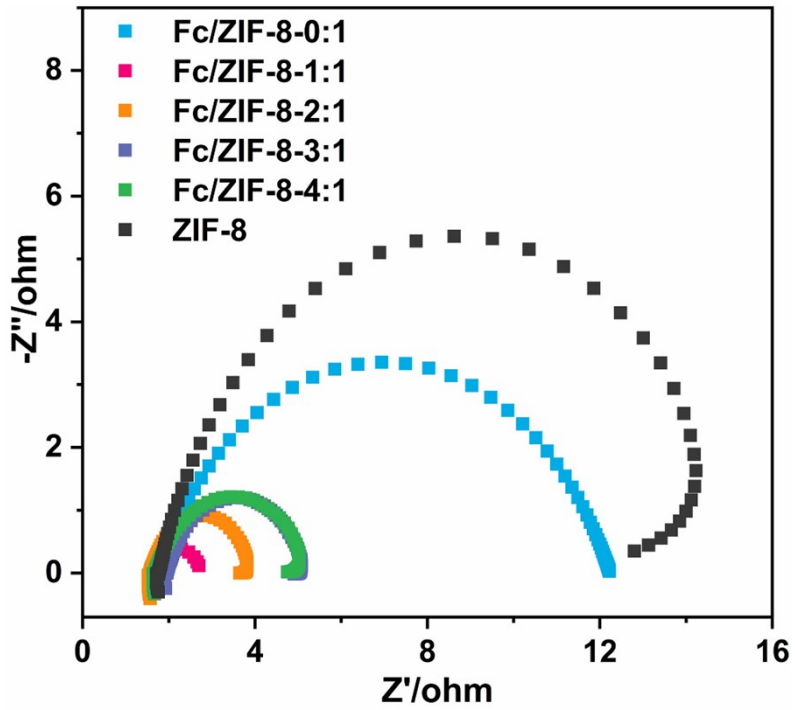

Fig. S18 Nyquist plots of Fc/ZIF-8-0:1, Fc/ZIF-8-1:1, Fc/ZIF-8-2:1, Fc/ZIF-8-3:1, Fc/ZIF-8-4:1 and ZIF-8.

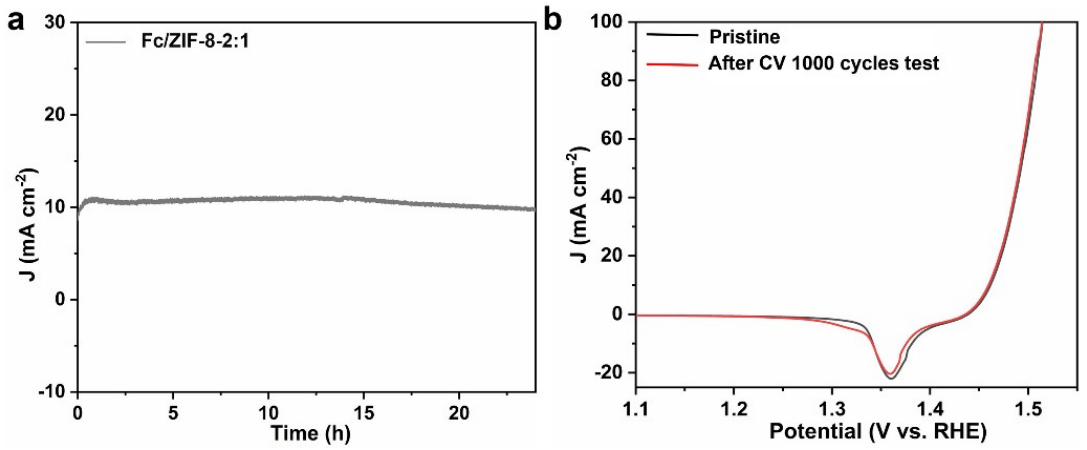

Fig. S19 The chronoamperometry curve at 10 mA cm^{-2} of Fc/ZIF-8-2:1 (a), and LSV curves of Fc/ZIF-8-2:1 before and after 1000 CV cycles (b).

Supplementary References

1. L. Zhong, X. Wang, Y. Guo, J. Ding, Q. Huang, T.-T. Li, Y. Hu, J. Qian and S. Huang, Differentiated oxygen evolution behavior in MOF-derived oxide nanomaterials induced by phase transition, *ACS Appl. Mater. Interfaces*, 2021, **13**, 55454-55462.

2. F.-L. Li, P. Wang, X. Huang, D. J. Young, H.-F. Wang, P. Braunstein and J.-P. Lang, Large-scale, bottom-up synthesis of binary metal-organic framework nanosheets for efficient water oxidation, *Angew. Chem. Int. Ed.*, 2019, **58**, 7051-7056.

3. J. Ma, S. Wang, W. He, H. Chen, X. Zhai, F. Meng and Y. Fu, Synthesis of FeNiCo ternary hydroxides through green grinding method with metal-organic frameworks as precursors for oxygen evolution reaction, *ChemSusChem*, 2021, **14**, 5042-5048.

4. C. Pan, Z. Liu and M. Huang, 2D iron-doped nickel MOF nanosheets grown on nickel foam for highly efficient oxygen evolution reaction, *Appl. Surf. Sci.*, 2020, **529**, 147201-147207.

5. D. Xing, Y. Wang, P. Zhou, Y. Liu, Z. Wang, P. Wang, Z. Zheng, H. Cheng, Y. Dai and B. Huang, Co_3(hexaiminotriphenylene)$_2$: a conductive two-dimensional π-d

conjugated metal-organic framework for highly efficient oxygen evolution reaction, *Appl. Catal. B: Environ.*, 2020, **278**, 119295-119303.

6. Y. Guo, J. Tang, Z. Wang, Y. Sugahara and Y. Yamauchi, Hollow porous heterometallic phosphide nanocubes for enhanced electrochemical water splitting, *Small*, 2018, **14**, 1802442-1802449.

7. M. Liu, L. Kong, X. Wang, J. He, J. Zhang, J. Zhu and X.-H. Bu, Deciphering of advantageous electrocatalytic water oxidation behavior of metal-organic framework in alkaline media, *Nano Res.*, 2021, **14**, 4680-4688.

8. W. Cheng, X. F. Lu, D. Luan and X. W. Lou, NiMn-based bimetal-organic framework nanosheets supported on multi-channel carbon fibers for efficient oxygen electrocatalysis, *Angew. Chem. Int. Ed.*, 2020, **59**, 18234-18239.

9. X. Zhang, J. Luo, K. Wan, D. Plessers, B. Sels, J. Song, L. Chen, T. Zhang, P. Tang, J. R. Morante, J. Arbiol and J. Fransaer, From rational design of a new bimetallic MOF family with tunable linkers to OER catalysts, *J. Mater. Chem. A*, 2019, **7**, 1616-1628.

10. W. Cheng, Z.-P. Wu, D. Luan, S.-Q. Zang and X. W. Lou, Synergetic cobalt-copper-based bimetal-organic framework nanoboxes toward efficient electrochemical oxygen evolution, *Angew. Chem. Int. Ed.*, 2021, **60**, 26397-26402.

11. W. Chen, Y. Zhang, R. Huang, Y. Zhou, Y. Wu, Y. Hu and K. Ostrikov, Ni-Co hydroxide nanosheets on plasma-reduced Co-based metal-organic nanocages for electrocatalytic water oxidation, *J. Mater. Chem. A*, 2019, **7**, 4950-4959.

12. J. Gao, J. Cong, Y. Wu, L. Sun, J. Yao and B. Chen, Bimetallic hofmann-type metal-organic framework nanoparticles for efficient electrocatalysis of oxygen evolution reaction, *ACS Appl. Energy Materi.*, 2018, **1**, 5140-5144.

13 J. Kang, M. J. Lee, N. G. Oh, J. Shin, S. J. Kwon, H. Chun, S-J Kim, H. Yun, H. Jo, K. M. Ok, and J. Do, I^3O^0-Type 3D Framework of Cobalt Cinnamate and Its Efficient Electrocatalytic Activity toward the Oxygen Evolution Reaction, *Chem. Mater.*, 2021, **33**, 2804-2813.

14 Y. Xu, W. Tu, B. Zhang, S. Yin, Y. Huang, M. Kraft, and R. Xu, Nickel Nanoparticles Encapsulated in Few-Layer Nitrogen-Doped Graphene Derived from

Metal-Organic Frameworks as Efficient Bifunctional Electrocatalysts for Overall Water Splitting, *Adv. Mater.*, 2017, **29**, 1605957.

15 J. Liang, X. Gao, B. Guo, Y. Ding, J. Yan, Z. Guo, E. C. M. Tse, and J. Liu, Ferrocene-Based Metal-Organic Framework Nanosheets as a Robust Oxygen Evolution Catalyst, *Angew. Chem. Int. Ed*., 2021, **60**, 12770-12774.

16 Q. Zhang, Y. Wang, Y. Wang, S. Yang, X. Wu, B. Lv, N.Wang, Y. Gao, X. Xu, H. Lei, R. Cao, Electropolymerization of cobalt porphyrins and corroles for the oxygen evolution reaction, *Chin. Chem. Lett.*, 2021, **32**, 3807-3810.

17 H. Qin, Y. Wang, B. Wang, X. Duan, H. Lei, X. Zhang, H. Zheng, W. Zhang, R. Cao, Cobalt porphyrins supported on carbon nanotubes as model catalysts of metal-N_4/C sites for oxygen electrocatalysis, *J. Energy Chem.*, 2021, 53, 77-81.